

Boosting All-in-One Image Restoration via Self-Improved Privilege Learning

Gang Wu

Harbin Institute of Technology
gwu@hit.edu.cn

Junjun Jiang*

Harbin Institute of Technology
jiangjunjun@hit.edu.cn

Kui Jiang

Harbin Institute of Technology
jiangkui@hit.edu.cn

Xianming Liu

Harbin Institute of Technology
csxm@hit.edu.cn

Abstract

Unified image restoration models for diverse and mixed degradations often suffer from unstable optimization dynamics and inter-task conflicts. This paper introduces Self-Improved Privilege Learning (SIPL), a novel paradigm that overcomes these limitations by innovatively extending the utility of privileged information (PI) beyond training into the inference stage. Unlike conventional Privilege Learning, where ground-truth-derived guidance is typically discarded after training, SIPL empowers the model to leverage its own preliminary outputs as *pseudo-privileged signals* for iterative self-refinement at test time. Central to SIPL is Proxy Fusion, a lightweight module incorporating a learnable Privileged Dictionary. During training, this dictionary distills essential high-frequency and structural priors from privileged feature representations. Critically, at inference, the *same* learned dictionary then interacts with features derived from the model’s initial restoration, facilitating a self-correction loop. SIPL can be seamlessly integrated into various backbone architectures, offering substantial performance improvements with minimal computational overhead. Extensive experiments demonstrate that SIPL significantly advances the state-of-the-art on diverse all-in-one image restoration benchmarks. For instance, when integrated with the PromptIR model, SIPL achieves remarkable PSNR improvements of +4.58 dB on composite degradation tasks and +1.28 dB on diverse five-task benchmarks, underscoring its effectiveness and broad applicability. Codes are available at our project page <https://github.com/Aitical/SIPL/tree/main>.

1 Introduction

Image restoration, a fundamental task within computer vision, seeks to reconstruct high-quality (HQ) images from degraded observations Banham and Katsaggelos [1997], Su et al. [2022-05]. Recently, the research community has increasingly focused on *all-in-one* image restoration methods, designed to address multiple degradation types with a unified model Jiang et al. [2024]. Despite their significant practical value, consolidating diverse restoration capabilities into a single network introduces substantial optimization challenges. Consistent with previous studies Kong et al. [2024], Wu et al. [2024], the all-in-one restoration task, typically a complex multi-task learning problem, is notably vulnerable to inter-task conflicts and negative transfer phenomena. Why does this occur? The core issue lies in the fundamental incompatibility between shared feature representations and task-specific requirements across different degradation types. For instance, the optimal feature

*Corresponding author.

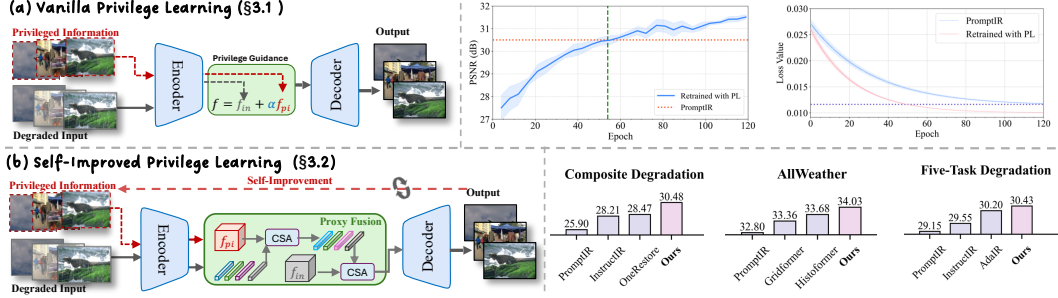


Figure 1: Conceptual comparison of learning frameworks: (a) Privilege Learning (PL) leverages privileged information during training for improved optimization. (b) Our proposed Self-Improved Privilege Learning (SIPL) framework introduces Proxy Fusion to retain privileged knowledge, enabling iterative self-refinement during inference by using intermediate restoration outputs as pseudo-privileged information. Retrained PromptIR with the proposed SIPL achieves significant improvement across diverse all-in-one tasks.

representations for denoising (focusing on local texture patterns) may fundamentally differ from those required for dehazing (emphasizing global atmospheric light estimation). When forced to share network parameters, gradients originating from these distinct tasks often conflict, causing certain tasks, particularly those with larger gradient magnitudes or simpler optimization landscapes, to dominate the training process. This dynamic consequently results in imbalanced convergence rates and diminished overall performance.

To address this fundamental limitation, we draw inspiration from Privilege Learning (PL) Vapnik and Vashist [2009], Vapnik et al. [2015]. We propose that privileged information, specifically GT-derived supervisory signals, can mitigate these adverse effects. The incorporation of privileged information during training establishes an *inter-task comprehension bridge*, effectively harmonizing conflicting gradients and stabilizing convergence. For instance, when we validated a PL-informed training framework on the PromptIR model, it not only achieved performance comparable to the original baseline in less than half the training epochs but also ultimately demonstrated significantly superior results. As illustrated in Figure 1(a), this form of privileged guidance demonstrably stabilizes the multi-task learning process, accelerates overall convergence, and enhances generalization across diverse degradation types. Introducing PL therefore presents an efficient and straightforward strategy for improving existing all-in-one restoration methods. Nevertheless, vanilla PL traditionally limits its own impact, as the privileged guidance is often progressively diminished during training and is entirely unavailable at inference time.

In this paper, we identify a critical, often overlooked opportunity: retaining the essence of privileged information to enhance inference-time performance. Addressing this key limitation, we propose the novel *Self-Improved Privilege Learning (SIPL)* framework (illustrated in Figure 1(b)). SIPL significantly extends traditional PL paradigms by enabling the model to leverage its intermediate restoration outputs as *pseudo-privileged information*, thereby introducing an iterative self-enhancement mechanism that actively refines performance during inference. Central to our SIPL approach is the effective *Proxy Fusion* mechanism, which employs a set of learnable parameters termed the *Privileged Dictionary*. Unlike vanilla PL strategies that directly blend privileged and primary features, Proxy Fusion exploits cross-attention to distill high-quality image priors from GT-derived privileged features during training. Critically, the learned Privileged Dictionary persists beyond the training phase. At inference, initial restoration outputs, although imperfect, inherently contain structural information significantly closer to the GT than the original degraded inputs. These outputs subsequently serve as pseudo-privileged information, iteratively interacting with this pre-learned Privileged Dictionary. This iterative refinement progressively improves internal feature representations, facilitating continuous, self-driven enhancement. The efficacy of this approach is evident from our validations: when integrated with the PromptIR model, SIPL yields substantial improvements across multiple all-in-one image restoration benchmarks, achieving PSNR gains of +4.58 dB on Composite Degradation, +1.23 dB on Allweather, and +1.38 dB on the Five-Task settings.

Our primary contributions are summarized as follows:

- We analyze the optimization impediments in all-in-one image restoration and establish the efficacy of Privilege Learning as a potent foundational strategy, demonstrating its ability to mitigate task competition and improve multi-task convergence.

- We propose the novel Self-Improved Privilege Learning (SIPL) framework, which uniquely extends PL to enable iterative self-improvement during inference.
- We introduce the Proxy Fusion module to efficiently distill and retain knowledge from privileged information. This plug-and-play mechanism adds minimal computational overhead while providing substantial quality improvements when integrated with various backbone restoration architectures.

2 Related Work

2.1 All-in-One Image Restoration

Traditional image restoration typically targets specific degradations, such as noise or blur, using specialized models Zamir et al. [2022], Huang et al. [2023], Cai et al. [2023]. However, real-world scenarios often involve unknown or mixed degradations, driving the need for *all-in-one* models that handle diverse degradation types in a unified framework Su et al. [2022-05], Jiang et al. [2024].

Early efforts toward unified models utilized powerful backbones Chen et al. [2022, 2021], Wang et al. [2022], Zamir et al. [2022], Wang et al. [2024], Guo et al. [2024a] or generative approaches like diffusion models Belhasin et al. [2024], Yue and Loy [2024], Li et al. [2025], Yue et al. [2025]. A key challenge is guiding a single network to handle diverse restoration tasks, leading to a focus on conditioning mechanisms, from early degradation encoders Li et al. [2022] to advanced learnable prompts Potlapalli et al. [2023], sometimes refined with frequency priors or dimensionality reduction Cui et al. [2025], Zhang et al. [2023]. Other methods use degradation priors from classifiers Kong et al. [2024] or vision-language models like CLIP with textual prompts Luo et al. [2024], Lin et al. [2024]. Additionally, multi-task learning techniques Wu et al. [2024, 2025] and pretraining strategies Qin et al. [2024] address optimization challenges. While these advances improve all-in-one capabilities, they often focus on architectural or input conditioning changes, overlooking optimization stability in multi-task learning.

2.2 Privilege Learning

Privilege Learning (PL), formally introduced as Learning Using Privileged Information (LUPI) Vapnik and Vashist [2009], Vapnik et al. [2015], is a machine learning paradigm where auxiliary information, inaccessible during inference, is provided to the model during training. This privileged information acts as a form of expert guidance, aiming to simplify the learning task, improve convergence, or enhance generalization, even though the model must perform inference without it. The core concept is that this richer training signal can help the model learn a more robust internal representation or decision boundary.

3 Method

In this section, we present our Self-Improved Privilege Learning (SIPL) framework for all-in-one image restoration. We first establish the foundational Privilege Learning (PL) paradigm to image restoration. We then introduce our novel SIPL, which uniquely enables self-improvement during inference through our proposed Proxy Fusion mechanism.

3.1 Privilege Learning

As established in Section 1, all-in-one image restoration faces fundamental optimization challenges stemming from task competition and conflicting gradient directions. Privilege Learning Vapnik and Vashist [2009], Vapnik et al. [2015] offers an elegant solution by leveraging additional information during training that enhances the learning process. Given a degraded image I_d and its corresponding ground truth I_{gt} , PL incorporates privileged information (derived from I_{gt}) into the training process. This is achieved through a simple yet effective feature fusion approach:

$$F_{fused} = (1 - \alpha) \cdot F_d + \alpha \cdot F_{PI}, \quad (1)$$

where F_d represents features extracted from the degraded image, F_{PI} denotes features derived from the ground truth (privileged information), and $\alpha \in [0, 1]$ controls the degree of privileged guidance. During training, α typically follows a decreasing schedule, ensuring the model gradually adapts to operating without privileged guidance. At inference time, α is set to 0, as privileged information is unneeded.

This straightforward mechanism provides substantial benefits for all-in-one restoration. It stabilizes training and mitigates task competition by providing clear guidance, particularly for challenging degradation types. Meanwhile, our introduced PL paradigm remains agnostic to model architecture, enhancing all-in-one image restoration generally.

3.2 Self-Improved Privilege Learning

Beyond the vanilla PL paradigm, we propose a novel extension to retain the privileged information at the inference stage. Our key insight is that the restoration output, though imperfect, contains valuable information closer to the ground truth than the original degraded input. This observation motivates our proxy fusion module, which enables the model to leverage its own outputs as pseudo-privileged information during inference.

Proxy Fusion The cornerstone of SIPL is our novel Proxy Fusion mechanism, which creates a persistent bridge between training-time privileged knowledge and inference-time self-improvement. Unlike the direct feature blending in conventional PL (Eq. 1), Proxy Fusion employs a learnable Privileged Dictionary (PD) to distill and retain essential knowledge from privileged information:

$$\text{PD} \in \mathbb{R}^{N \times C}, \quad (2)$$

where N represents the number of dictionary entries and C is the feature dimension. This dictionary interacts with privileged features through cross-attention:

$$F'_{PI} = \text{CrossAttention}(Q = \text{PD}, K = F_{PI}, V = F_{PI}), \quad (3)$$

This interaction allows the PD to capture and internalize high-frequency details and statistical patterns characteristic of high-quality images. The distilled knowledge is then integrated with features from the degraded image:

$$F_{fused} = \text{CrossAttention}(Q = F_d, K = F'_{PI}, V = F'_{PI}). \quad (4)$$

During training, the entire framework, including the Privileged Dictionary, learns to extract and utilize privileged information effectively. Crucially, the learned PD persists into inference, serving as a knowledge repository that enables self-improvement without requiring actual ground truth.

Self-Improvement Mechanism The distinguishing feature of SIPL is its iterative self-refinement capability during inference:

1. **Initial Restoration:** The model produces an initial output $I_{restored}^{(0)}$ using only the degraded input:

$$I_{restored}^{(0)} = \mathcal{F}(I_d). \quad (5)$$

2. **Self-Improvement:** This initial output serves as pseudo-privileged information. Features extracted from $I_{restored}^{(0)}$ interact with the learned PD through the Proxy Fusion mechanism, guiding subsequent restoration:

$$I_{restored}^{(1)} = \mathcal{F}(I_d, I_{restored}^{(0)}). \quad (6)$$

3. **Iterative Refinement (Optional):** This process can continue for multiple iterations, with each step potentially improving quality:

$$I_{restored}^{(t)} = \mathcal{F}(I_d, I_{restored}^{(t-1)}), \quad t \geq 1. \quad (7)$$

This elegant self-correction loop enables progressive quality enhancement without requiring actual ground truth during deployment. In practice, we find that a single refinement step ($t = 1$) typically provides substantial improvements with minimal computational overhead.

The key advantage of our Proxy Fusion approach over direct feature blending is its ability to distill and retain essential high-quality image characteristics in the learned PD parameters. This creates a persistent knowledge repository that facilitates self-improvement during inference, a capability absent in conventional PL frameworks.

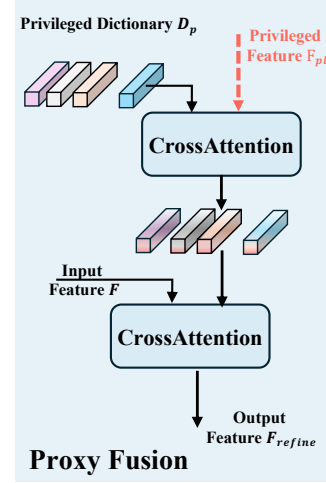


Figure 2: Implementation of the proxy fusion module.

Table 1: Quantitative results (PSNR/SSIM) on the Three-Task Setting. Our results are highlighted in **bold**, and best results are underlined.

| Type | Method | Venue | Denoising (BSD68) | | | Dehazing | Deraining | Average |
|------------|------------------------------------|------------|--------------------|--------------------|--------------------|--------------------|--------------------|--------------------|
| | | | $\sigma = 15$ | $\sigma = 25$ | $\sigma = 50$ | SOTS | Rain100L | |
| General | MPRNet Zamir et al. [2021] | CVPR'21 | 33.27/0.920 | 30.76/0.871 | 27.29/0.761 | 28.00/0.958 | 33.86/0.958 | 30.63/0.894 |
| | Restormer Zamir et al. [2022] | CVPR'22 | 33.72/0.930 | 30.67/0.865 | 27.63/0.792 | 27.78/0.958 | 33.78/0.958 | 30.75/0.901 |
| | NAFNet Chen et al. [2022] | ECCV'22 | 33.03/0.918 | 30.47/0.865 | 27.12/0.754 | 24.11/0.928 | 33.64/0.956 | 29.67/0.844 |
| | FSNet* Cui et al. [2022] | TPAMI'23 | 33.81/0.930 | 30.84/0.872 | 27.69/0.792 | 29.14/0.968 | 35.61/0.969 | 31.42/0.906 |
| | DRSformer* Chen et al. [2023] | CVPR'23 | 33.28/0.921 | 30.55/0.862 | 27.58/0.786 | 29.02/0.968 | 35.89/0.970 | 31.26/0.902 |
| | MambaIR* Guo et al. [2024a] | ECCV'24 | 33.88/0.931 | 30.95/0.874 | 27.74/0.793 | 29.57/0.970 | 35.42/0.969 | 31.51/0.907 |
| All-in-One | DL Fan et al. [2019] | TPAMI'19 | 33.05/0.914 | 30.41/0.861 | 26.90/0.740 | 26.92/0.391 | 32.62/0.931 | 29.98/0.875 |
| | AirNet Li et al. [2022] | CVPR'22 | 33.92/0.932 | 31.26/0.888 | 28.00/0.797 | 27.94/0.962 | 34.90/0.967 | 31.20/0.910 |
| | IDR* Zhang et al. [2023] | CVPR'23 | 33.89/0.931 | 31.32/0.884 | 28.04/0.798 | 29.87/0.970 | 36.03/0.971 | 31.83/0.911 |
| | Gridformer* Wang et al. [2024] | IJCV'24 | 33.93/0.931 | 31.37/0.887 | 28.11/0.801 | 30.37/0.970 | 37.15/0.972 | 32.19/0.912 |
| | NDR Yao et al. [2024] | TIP'24 | 34.01/0.932 | 31.36/0.887 | 28.10/0.798 | 28.64/0.962 | 35.42/0.969 | 31.51/0.910 |
| | InstructIR Conde et al. [2024] | ECCV'24 | 34.15/0.933 | 31.52/0.890 | <u>28.30/0.804</u> | 30.22/0.959 | 37.98/0.978 | 32.43/0.913 |
| | TextualDegRemovalLin et al. [2024] | CVPR'24 | 34.01/0.933 | 31.39/0.890 | 28.18/0.802 | <u>31.63/0.980</u> | 37.58/0.979 | 32.63/0.917 |
| | AdaIR Cui et al. [2025] | ICLR'25 | 34.12/0.935 | 31.45/0.892 | 28.19/0.802 | 31.06/0.980 | 38.64/0.983 | <u>32.69/0.918</u> |
| | PromptIR Potlapalli et al. [2023] | NeurIPS'23 | 33.98/0.933 | 31.31/0.888 | 28.06/0.799 | 30.58/0.974 | 36.37/0.972 | 32.06/0.913 |
| | PromptIR + SIPL | 2025 | 34.12/0.933 | 31.48/0.889 | 28.22/0.800 | 31.09/0.977 | 38.43/0.984 | 32.67/0.917 |

3.3 Remarks

Our SIPL framework focuses exclusively on the learning paradigm rather than specific architectural choices. The Proxy Fusion module serves as a plug-and-play component that can enhance virtually any existing restoration architecture. This architectural agnosticism ensures broad applicability across diverse restoration models and tasks. For experimental validation, we integrate SIPL into multiple distinct backbone architectures, including PromptIR Potlapalli et al. [2023]. As demonstrated in Section 4, SIPL consistently improves performance across all tested models, confirming its generality and effectiveness as an optimization framework for all-in-one image restoration.

4 Experiments

In this section, we conduct extensive experiments to evaluate our Self-Improved Privilege Learning (SIPL) framework across various all-in-one image restoration settings. We first describe our experimental setup, implementation details, and evaluation metrics. Then, we present quantitative and qualitative comparisons with state-of-the-art methods, followed by comprehensive ablation studies that validate the effectiveness of our key components.

4.1 Experimental Setup

We evaluate SIPL across five comprehensive all-in-one settings that encompass a wide range of real-world image degradation scenarios:

- Three-Task Setting:** Following the established protocol in Li et al. [2022], Potlapalli et al. [2023], we address three distinct degradation tasks: image denoising (with synthetic Gaussian noise), deraining (using the Rain100L dataset), and dehazing (on the RESIDE dataset). For denoising, we use BSD400 Arbeláez et al. [2011] and WED Ma et al. [2017] for training, and test on BSD68 with noise levels of 15, 25, and 50. For deraining, we employ the Rain100L Yang et al. [2017] dataset, and for dehazing, we use the outdoor subset of RESIDE Li et al. [2019a].
- Five-Task Setting:** To evaluate our model’s capacity to handle a broader spectrum of degradations, we utilize a five-task benchmark, including deraining (Rain100L Yang et al. [2017]), dehazing (RESIDE Indoor Training Set), denoising (BSD400 + WED), motion deblurring (GoPro Nah et al. [2017]), and low-light enhancement (LOL Wei et al. [2018]). This setting follows Zhang et al. [2023] and tests the model’s ability to handle diverse degradation types in real-world scenarios.
- Deweathering Setting:** Based on previous work Valanarasu et al. [2022], we use the AllWeather Valanarasu et al. [2022] dataset for training, containing images from Raindrop Qian et al. [2018], Outdoor-Rain Li et al. [2019b], and Snow100K Liu et al. [2018].
- Composite Degradation Setting:** Following the protocol established in Guo et al. [2024b], we evaluate our method on the Composite Degradation Dataset (CDD-11), which represents a more challenging scenario with mixed degradations. CDD-11 encompasses 11 categories of image degradations including single degradations (low-light, haze, rain, snow) and their combinations (low+haze, low+rain, low+snow, haze+rain, haze+snow, low+haze+rain, low+haze+snow). The dataset is constructed using standard benchmarks: the LOW-Light

Table 2: Quantitative results (PSNR/SSIM) on the Five-Task Setting. Our results are highlighted in **bold**, and best results are underlined.

| Type | Method | Venue | Denoising | Dehazing | Deraining | Deblurring | Low-light | Average |
|------------|---------------------------------------|------------|--------------------|--------------------|--------------------|--------------------|--------------------|--------------------|
| | | | BSD68 | SOTS | Rain100L | GoPro | LOL | |
| General | SwinIR Liang et al. [2021] | ICCVW'21 | 30.59/0.868 | 21.50/0.891 | 30.78/0.923 | 24.52/0.773 | 17.81/0.723 | 25.04/0.835 |
| | Restormer Zamir et al. [2022] | CVPR'22 | 31.49/0.884 | 24.09/0.927 | 34.81/0.962 | 27.22/0.829 | 20.41/0.806 | 27.60/0.881 |
| | NAFNet Chen et al. [2022] | ECCV'22 | 31.02/0.883 | 25.23/0.939 | 35.56/0.967 | 26.53/0.808 | 20.49/0.809 | 27.76/0.881 |
| | DRSformer* Chen et al. [2023] | CVPR'23 | 30.97/0.881 | 24.66/0.931 | 33.45/0.953 | 25.56/0.780 | 21.77/0.821 | 27.28/0.873 |
| | Retinexformer* Cai et al. [2023] | ICCV'23 | 30.84/0.880 | 24.81/0.933 | 32.68/0.940 | 25.09/0.779 | 22.76/0.834 | 27.24/0.873 |
| | FSNet* Cui et al. [2024] | TPAMI'23 | 31.33/0.883 | 25.53/0.943 | 36.07/0.968 | 28.32/0.869 | 22.29/0.829 | 28.71/0.898 |
| | MambaIR* Guo et al. [2024a] | ECCV'24 | 31.41/0.884 | 25.81/0.944 | 36.55/0.971 | 28.61/0.875 | 22.49/0.832 | 28.97/0.901 |
| All-in-One | DL Fan et al. [2019] | TPAMI'19 | 23.09/0.745 | 20.54/0.826 | 21.96/0.762 | 19.86/0.672 | 19.83/0.712 | 21.05/0.743 |
| | TAPE Liu et al. [2022] | ECCV'22 | 30.18/0.855 | 22.16/0.861 | 29.67/0.904 | 24.47/0.763 | 18.97/0.621 | 25.09/0.801 |
| | Transweather Valanarasu et al. [2022] | CVPR'22 | 29.00/0.841 | 21.32/0.885 | 29.43/0.905 | 25.12/0.757 | 21.21/0.792 | 25.22/0.836 |
| | AirNet Li et al. [2022] | CVPR'22 | 30.91/0.882 | 21.04/0.884 | 32.98/0.951 | 24.35/0.781 | 18.18/0.735 | 25.49/0.846 |
| | IDR Zhang et al. [2023] | CVPR'23 | <u>31.60/0.887</u> | 25.24/0.943 | 35.63/0.965 | 27.87/0.846 | 21.34/0.826 | 28.34/0.893 |
| | Gridformer* Wang et al. [2024] | IJCV'24 | 31.45/0.885 | 26.79/0.951 | 36.61/0.971 | 29.22/0.884 | 22.59/0.831 | 29.33/0.904 |
| | InstructIR Conde et al. [2024] | ECCV'24 | 31.40/0.887 | 27.10/0.956 | 36.84/0.973 | <u>29.40/0.886</u> | 23.00/0.836 | 29.55/0.907 |
| | AdaIR Cui et al. [2025] | ICLR'25 | 31.35/0.889 | <u>30.53/0.978</u> | 38.02/0.981 | 28.12/0.858 | 23.00/0.845 | 30.20/0.910 |
| | PromptIR* Potlapalli et al. [2023] | NeurIPS'23 | 31.47/0.886 | 26.54/0.949 | 36.37/0.970 | 28.71/0.881 | 22.68/0.832 | 29.15/0.904 |
| | PromptIR + SIPL | 2025 | 31.45/0.888 | 30.51/0.975 | 38.09/0.982 | 29.35/0.886 | 23.23/0.856 | 30.53/0.917 |

dataset (LOL) Wei et al. [2018], the REalistic Single Image DEhazing Outdoor Training Set (RESIDE-OTS) Li et al. [2019a], the Rain1200 dataset Zhang and Patel [2018], and the Snow100k dataset Liu et al. [2018]. This setting particularly evaluates our framework’s capability to handle complex, interacting degradations that better reflect real-world scenarios.

For all settings, we adopt the same training/testing splits and protocols as in the original works to ensure fair comparisons. We integrate our proposed SIPL framework into various backbone architectures to demonstrate its versatility and effectiveness.

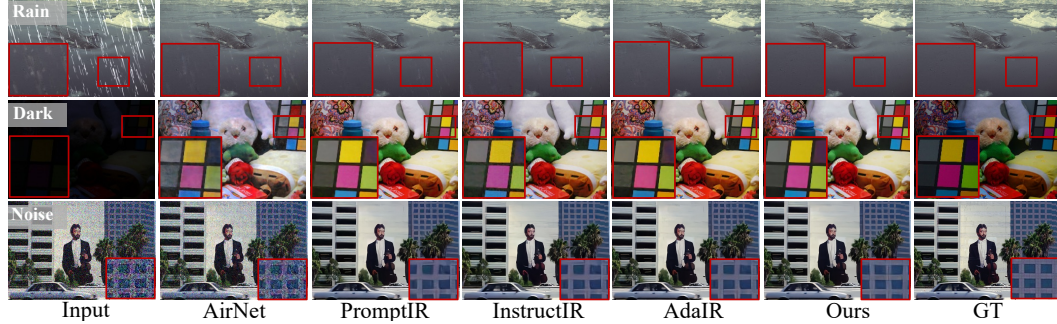


Figure 3: Visual comparison on the Five-Task benchmark. Our method demonstrates superior restoration quality across diverse degradations, effectively recovering finer details and image structures compared to other approaches.

4.2 Main Results

We now present the quantitative comparison of our SIPL framework, integrated with the PromptIR backbone (denoted as “PromptIR + SIPL”), against the original PromptIR and other state-of-the-art methods across the four benchmark settings.

Results on Three-Task Setting As presented in Table 1, PromptIR enhanced with our SIPL framework demonstrates marked improvements over the original baseline across all three degradation tasks. Specifically, our method achieves an average PSNR of 32.67 dB, a notable gain of +0.61 dB compared to the PromptIR. The advantages of SIPL are particularly evident in deraining, with a PSNR increase of +2.06 dB (38.43 dB vs. 36.37 dB), and dehazing, with a +0.51 dB PSNR improvement (31.09 dB vs. 30.58 dB). These results position our approach favorably against recent state-of-the-art all-in-one methods, including AdaIR Cui et al. [2025] and TextualDegRemoval Lin et al. [2024], establishing its strong competitiveness.

Results on Five-Task Setting Table 2 details the performance on the more comprehensive five-task benchmark. In this more demanding scenario, SIPL’s benefits are even more pronounced. Our retrained model achieves an average PSNR of 30.53 dB, significantly surpassing the PromptIR baseline by +1.38 dB. Substantial gains are observed across multiple tasks, notably in dehazing

Table 3: Quantitative results (PSNR/SSIM) on the Deweathering Setting. Our results are highlighted in **bold**, and best results are underlined.

| Method | Venue | Snow100K-S | | Snow100K-L | | Outdoor-Rain | | RainDrop | | Average | |
|------------------------------------------------------------|------------|--------------|---------------|--------------|---------------|--------------|---------------|--------------|---------------|--------------|---------------|
| | | PSNR | SSIM | PSNR | SSIM | PSNR | SSIM | PSNR | SSIM | PSNR | SSIM |
| All-in-One Li et al. [2020] | CVPR'20 | – | – | 28.33 | 0.8820 | 24.71 | 0.8980 | 31.12 | 0.9268 | 28.05 | 0.9023 |
| Transweather Valanarasu et al. [2022] | CVPR'22 | 32.51 | 0.9341 | 29.31 | 0.8879 | 28.83 | 0.9000 | 30.17 | 0.9157 | 30.20 | 0.9094 |
| WGSNet Zhu et al. [2023] | CVPR'22 | 34.31 | 0.9460 | 30.16 | 0.9007 | 29.32 | 0.9207 | 32.38 | 0.9378 | 31.54 | 0.9263 |
| WeatherDiff ₆₄ Özdenizci and Legenstein [2023] | TPAMI'23 | 35.83 | 0.9566 | 30.09 | 0.9041 | 29.64 | 0.9312 | 30.71 | 0.9312 | 31.57 | 0.9308 |
| WeatherDiff ₁₂₈ Özdenizci and Legenstein [2023] | TPAMI'23 | 35.02 | 0.9516 | 29.58 | 0.8941 | 29.72 | 0.9216 | 29.66 | 0.9225 | 31.00 | 0.9225 |
| AWRCP Ye et al. [2023] | ICCV'23 | 36.92 | 0.9652 | 31.92 | 0.9341 | 31.39 | 0.9329 | 31.93 | 0.9314 | 33.04 | 0.9409 |
| GridFormer Wang et al. [2024] | IJCV'24 | 37.46 | 0.9640 | 31.71 | 0.9231 | 31.87 | 0.9335 | 32.39 | 0.9362 | 33.36 | 0.9392 |
| MPerceiver Ai et al. [2024] | CVPR'24 | 36.23 | 0.9571 | 31.02 | 0.9164 | 31.25 | 0.9246 | 33.21 | 0.9294 | 32.93 | 0.9319 |
| DTPM Ye et al. [2024] | CVPR'24 | 37.01 | 0.9663 | 30.92 | 0.9174 | 30.99 | 0.9340 | 32.72 | 0.9440 | 32.91 | 0.9404 |
| Histoformer Sun et al. [2024] | ECCV'24 | 37.41 | 0.9656 | 32.16 | 0.9261 | 32.08 | 0.9389 | 33.06 | 0.9441 | 33.68 | 0.9437 |
| PromptIR Potlapalli et al. [2023] | NeurIPS'23 | 36.88 | 0.9643 | 31.34 | 0.9200 | 30.80 | 0.9229 | 32.20 | 0.9359 | 32.80 | 0.9357 |
| PromptIR + SIPL | 2025 | 37.91 | 0.9673 | 32.34 | 0.9291 | 32.91 | 0.9469 | 32.99 | 0.9462 | 34.03 | 0.9473 |

(+3.97 dB PSNR, 30.51 dB vs. 26.54 dB), deraining (+1.72 dB PSNR, 38.09 dB vs. 36.37 dB), and low-light enhancement (+0.55 dB PSNR, 23.23 dB vs. 22.68 dB). Moreover, our SIPL-augmented model consistently outperforms recent leading methods such as AdaIR Cui et al. [2025] and InstructIR Conde et al. [2024], setting a new state-of-the-art for this challenging multi-task evaluation. Visual comparisons, as illustrated in Figure 3, further corroborate these quantitative findings. Our SIPL-enhanced model consistently produces sharper images with better-preserved textures and structural details across the diverse range of degradations, effectively handling tasks from denoising to low-light enhancement where other methods may falter.

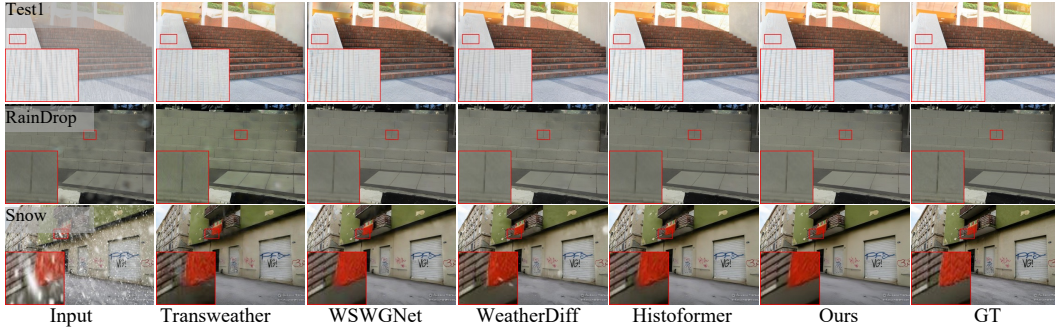


Figure 4: Qualitative examples from the AllWeather dataset. Our method exhibits robust performance in removing various challenging weather conditions. It yields visually superior results with better detail preservation and fewer artifacts.

Results on Deweathering Setting The deweathering benchmark, summarized in Table 3, evaluates performance on removing diverse adverse weather conditions. Our approach again demonstrates superior capabilities, achieving the new SOTA average PSNR of 34.03 dB and SSIM of 0.9473. This represents a significant +1.23 dB PSNR improvement over the PromptIR baseline. Consistent performance enhancements are recorded across all four test datasets. These results underscore SIPL’s robustness in complex deweathering scenarios, outperforming specialized methods and recent deweathering models like Histoformer Sun et al. [2024] and GridFormer Wang et al. [2024]. The qualitative results presented in Figure 4 further highlight the efficacy of our approach. Compared to existing deweathering methods, our retrained PromptIR more effectively removes various weather-related artifacts, such as dense haze and heavy rain, while better preserving image details and avoiding color casts, leading to visually cleaner and more faithful restorations.

Results on Composite Degradation Setting Table 4 evaluates performance on the highly challenging Composite Degradation Dataset (CDD-11), which features images with both single and multiple interacting degradations. Our proposed SIPL delivers outstanding results, achieving an average PSNR of 30.48 dB. This marks a substantial improvement of +4.58 dB over the original PromptIR baseline. This clearly demonstrates the significant contribution of the inference-time self-improvement mechanism, enabled by Proxy Fusion, beyond the benefits of PL-enhanced training alone. The performance leap is particularly remarkable for severe combined degradations: for instance, on haze+snow (h+s) and haze+rain (h+r), our approach achieves PSNR gains of +9.01 dB and +8.16 dB respectively,

Table 4: Quantitative results (PSNR/SSIM/LPIPS) on the Composite Degradation Setting. Our results are highlighted in **bold**, and best results are underlined.

| Method | Venue | l | h | r | s | l+h | l+r | l+s | h+r | h+s | l+h+r | l+h+s | Avg. |
|--------------------------------------------|------------|--------------|--------------|--------------|--------------|--------------|--------------|--------------|--------------|--------------|--------------|--------------|--------------|
| AirNetLi et al. [2022] | CVPR'22 | 24.83 | 24.21 | 26.55 | 26.79 | 23.23 | 22.82 | 23.29 | 22.21 | 23.29 | 21.80 | 22.24 | 23.75 |
| TransWeatherValanarasu et al. [2022] | CVPR'22 | 23.39 | 23.95 | 26.69 | 25.74 | 22.24 | 22.62 | 21.80 | 23.10 | 22.34 | 21.55 | 21.01 | 23.13 |
| WeatherDiffÖzdenizci and Legenstein [2023] | TPAMI'23 | 23.58 | 21.99 | 24.85 | 24.80 | 21.83 | 22.69 | 22.12 | 21.25 | 21.99 | 21.23 | 21.04 | 22.49 |
| WGWSNetZhu et al. [2023] | CVPR'23 | 24.39 | 27.90 | 33.15 | 34.43 | 24.27 | 25.06 | 24.60 | 27.23 | 27.65 | 23.90 | 23.97 | 26.96 |
| InstructIRConde et al. [2024] | ECCV'24 | 26.70 | 32.61 | 33.51 | 34.45 | 24.36 | 25.41 | 25.63 | 28.80 | 29.64 | 24.84 | 24.32 | 28.21 |
| OneRestoreGuo et al. [2024b] | ECCV'24 | 26.55 | 32.71 | 33.48 | 34.50 | 26.15 | 25.83 | 25.56 | 30.27 | 30.46 | 25.18 | 25.28 | 28.47 |
| PromptIRPotlapalli et al. [2023] | NeurIPS'23 | 26.32 | 26.10 | 31.56 | 31.53 | 24.49 | 25.05 | 24.51 | 24.54 | 23.70 | 23.74 | 23.33 | 25.90 |
| PromptIR + SIPL | 2025 | 27.62 | 36.82 | 35.66 | 36.85 | 27.03 | 26.79 | 26.68 | 32.70 | 32.71 | 26.20 | 26.20 | 30.48 |

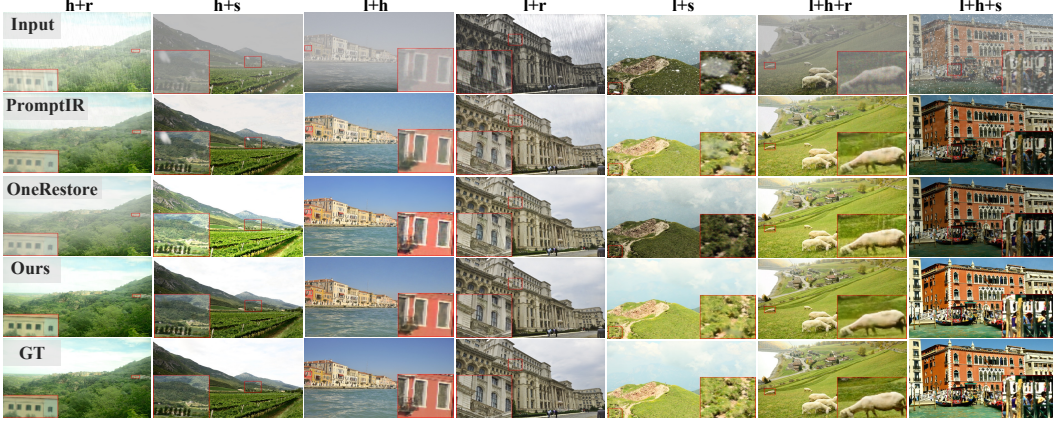


Figure 5: Visual results on the composite degradation tasks, showcasing performance on mixed degradations. Our method more effectively mitigates multiple interacting degradations, restoring clearer images with improved color fidelity and detail.

over the baseline PromptIR. Similarly, for triple degradations such as low-light+haze+snow (l+h+s) and low-light+haze+rain (l+h+r), the improvements are +2.87 dB and +2.46 dB, respectively. Our method also significantly surpasses other recent models designed for composite degradations, such as OneRestore Guo et al. [2024b] and InstructIR Conde et al. [2024]. Figure 5 provides compelling visual evidence of SIPL’s advantages on the composite degradation tasks. In scenarios with multiple co-occurring degradations, baseline methods like PromptIR and OneRestore sometimes struggle. For instance with low + snow degradation, they address only one degradation, appearing to remove snow but failing to correct the low-light induced color cast or restore details in dark regions. In contrast, our method demonstrates superior accuracy and generalization.

4.3 Ablation Studies

In this section, we conduct comprehensive ablation studies to meticulously validate the efficacy of our proposed Self-Improved Privilege Learning framework and dissect the contributions of its core components.

Architectural Agnosticism of SIPL A core strength of our SIPL framework lies in its architectural agnosticism and ease of integration. To substantiate this plug-and-play capability, we applied SIPL to a spectrum of distinct backbone architectures, moving beyond the PromptIR Potlapalli et al. [2023]. These included Restormer Zamir et al. [2022], a prominent Transformer-based network; NAFNet Chen et al. [2022], known for its high CNN efficiency; and AdaIR Cui et al. [2025], a recent state-of-the-art method notable for its frequency domain processing. All models were re-

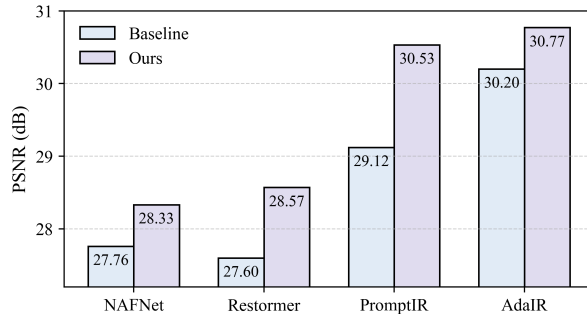


Figure 6: Ablation study on the interaction of SIPL with diverse backbone architectures on the five-task benchmark. “Original” refers to the baseline model, and “Ours” refers to the baseline model augmented with our SIPL framework. SIPL consistently improves performance across different architectures.

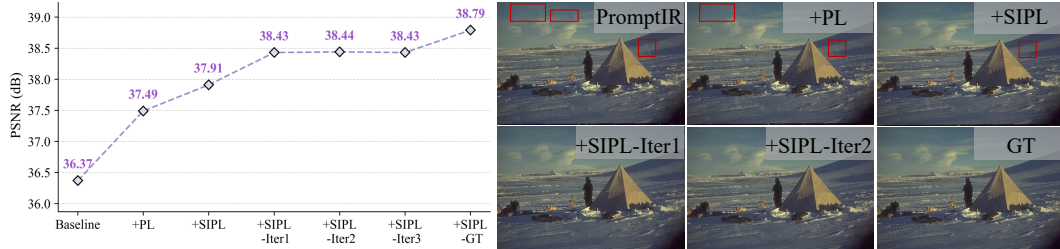


Figure 7: Ablation study dissecting the contributions of SIPL’s components. The figure illustrates the progressive improvements from the baseline, through the addition of privilege learning (“+PL”), the initial application of SIPL (“+SIPL”), and subsequent iterative self-refinement stages (“+SIPL-IterX”). Performance is benchmarked against an approximate upper bound using GT-guidance (“+SIPL-GT”).

trained on the five-task benchmark (as detailed in Section 4.1) with and without the SIPL framework integrated. The results, presented in Figure 6, unequivocally showcase SIPL’s ability to consistently elevate performance across these diverse architectural paradigms. Specifically, integrating SIPL boosted NAFNet’s average PSNR from 27.76 dB to 28.33 dB and Restormer’s from 27.60 dB to 28.57 dB. The PromptIR model itself saw its performance climb from 29.12 dB to 30.53 dB. Even for a strong baseline like AdaIR, SIPL provided a further enhancement, increasing its average PSNR from 30.20 dB to 30.77 dB. These consistent improvements across varied models underscore SIPL’s versatility as a general learning framework, not tightly coupled to any specific architecture, that effectively refines model optimization and enables potent inference-time self-improvement.

Dissecting the Contributions of SIPL Components To meticulously evaluate SIPL’s core components, we ablate PromptIR on a five degradation tasks, with quantitative and qualitative results presented in Figure 7. The baseline PromptIR model achieves a PSNR of 36.37 dB. Introducing privilege learning solely during training (“+PL”) substantially boosts performance to 37.49 dB. This underscores PL’s efficacy in stabilizing multi-task optimization by leveraging privileged information, thereby establishing a stronger foundation. Building upon this, the full SIPL framework, by incorporating the Proxy Fusion module for its initial inference application (“+SIPL”), further elevates the PSNR to 37.91 dB (+0.42 dB over “+PL”). This increment highlights the Proxy Fusion module’s critical role, with its Privileged Dictionary, in effectively distilling, preserving, and transferring privileged knowledge for tangible improvement at inference time. The iterative self-improvement mechanism, a key innovation of SIPL, demonstrates further significant refinement. Crucially, when the model’s output from the “+SIPL” stage is *first fed back as pseudo-privileged information* (resulting in “+SIPL-Iter1”), performance impressively surges to 38.43 dB—an additional +0.52 dB gain. This substantial improvement from the initial feedback loop powerfully demonstrates the innovation and effectiveness of using self-generated outputs for refinement. While subsequent iterations show diminishing returns, they affirm the model’s capacity for self-correction. This iterative process using pseudo-PI effectively narrows the gap towards the performance upper bound of 38.79 dB, achieved when utilizing true ground truth as privileged input during inference.

4.4 Limitation and Future Work

Our extensive experiments and ablation studies have demonstrated the significant success of the proposed SIPL framework. Nevertheless, we identify key areas and challenges that warrant further investigation. A key consideration is the computational cost of iterative refinement. While iterations significantly boost performance (as shown in Figure 7), they add inference latency. Although SIPL’s initial single-pass application is already potent, future work could focus on optimizing prior distillation and utilization to maximize this initial-pass efficacy. Additionally, the performance gap to GT-guided inference underscores the gap of current pseudo-privileged information, which may not fully align with true privileged priors. Thus, improving pseudo-PI fidelity and its alignment with ground truth remains a critical research direction for pushing restoration boundaries. Finally, a more comprehensive theoretical understanding of SIPL’s self-improvement convergence is essential for advancing the robustness and broader applicability of all-in-one restoration.

5 Conclusion

In this work, we propose Self-Improved Privilege Learning (SIPL), a novel framework that effectively tackles critical optimization impediments in all-in-one image restoration. SIPL uniquely extends the paradigm of privilege learning to the inference stage: models are empowered to iteratively self-refine their outputs by leveraging them as pseudo-privileged information. This is realized through our

proposed proxy fusion module, which employs a privileged dictionary, distilled from ground-truth priors during training, to guide this self-correction process with retrained privileged prior. Extensive evaluations across multiple challenging benchmarks, particularly those with complex composite degradations, confirm that SIPL substantially boosts the performance of diverse state-of-the-art methods, significantly enhancing their robustness and overall restoration quality. We hope that the principles and methodologies presented in SIPL will offer fresh perspectives to the community and stimulate further exploration into more effective strategies for all-in-one image restoration.

References

- M.R. Banham and A.K. Katsaggelos. Digital image restoration. *IEEE Signal Processing Magazine*, 14(2):24–41, 1997.
- Jingwen Su, Boyan Xu, and Hujun Yin. A survey of deep learning approaches to image restoration. *Neurocomput.*, 487:46–65, 2022-05. ISSN 0925-2312.
- Junjun Jiang, Zengyuan Zuo, Gang Wu, Kui Jiang, and Xianming Liu. A survey on all-in-one image restoration: Taxonomy, evaluation and future trends. *CoRR*, abs/2410.15067, 2024.
- Xiangtao Kong, Chao Dong, and Lei Zhang. Towards effective multiple-in-one image restoration: A sequential and prompt learning strategy. *CoRR*, abs/2401.03379, 2024.
- Gang Wu, Junjun Jiang, Kui Jiang, and Xianming Liu. Harmony in diversity: Improving all-in-one image restoration via multi-task collaboration. In *ACM Multimedia*, pages 6015–6023, 2024.
- Vladimir Vapnik and Akshay Vashist. A new learning paradigm: Learning using privileged information. *Neural networks*, 22(5-6):544–557, 2009.
- Vladimir Vapnik, Rauf Izmailov, et al. Learning using privileged information: similarity control and knowledge transfer. *J. Mach. Learn. Res.*, 16(1):2023–2049, 2015.
- Syed Waqas Zamir, Aditya Arora, Salman Khan, Munawar Hayat, Fahad Shahbaz Khan, and Ming-Hsuan Yang. Restormer: Efficient transformer for high-resolution image restoration. In *IEEE conference on computer vision and pattern recognition (CVPR)*, pages 5718–5729, 2022.
- Huaibo Huang, Mandi Luo, and Ran He. Memory uncertainty learning for real-world single image deraining. *IEEE Transactions on Pattern Analysis and Machine Intelligence*, 45(3):3446–3460, 2023.
- Yuanhao Cai, Hao Bian, Jing Lin, Haoqian Wang, Radu Timofte, and Yulun Zhang. Retinexformer: One-stage retinex-based transformer for low-light image enhancement. In *Proceedings of the IEEE/CVF international conference on computer vision (ICCV)*, pages 12470–12479, 2023.
- Liangyu Chen, Xiaojie Chu, Xiangyu Zhang, and Jian Sun. Simple baselines for image restoration. In *Proceedings of the european conference on computer vision (ECCV)*, volume 13667, pages 17–33, 2022.
- Hanting Chen, Yunhe Wang, Tianyu Guo, Chang Xu, Yiping Deng, Zhenhua Liu, Siwei Ma, Chunjing Xu, Chao Xu, and Wen Gao. Pre-trained image processing transformer. In *Proceedings of the IEEE/CVF conference on computer vision and pattern recognition (CVPR)*, pages 12299–12310, 2021.
- Zhendong Wang, Xiaodong Cun, Jianmin Bao, Wengang Zhou, Jianzhuang Liu, and Houqiang Li. Uformer: A general u-shaped transformer for image restoration. In *Proceedings of the IEEE conference on computer vision and pattern recognition (CVPR)*, pages 17662–17672, 2022.
- Tao Wang, Kaihao Zhang, Ziqian Shao, Wenhan Luo, Björn Stenger, Tong Lu, Tae-Kyun Kim, Wei Liu, and Hongdong Li. Gridformer: Residual dense transformer with grid structure for image restoration in adverse weather conditions. *Int. J. Comput. Vis.*, 132(10):4541–4563, 2024.
- Hang Guo, Jinmin Li, Tao Dai, Zhihao Ouyang, Xudong Ren, and Shu-Tao Xia. Mambair: A simple baseline for image restoration with state-space model. In *Proceedings of the european conference on computer vision (ECCV)*, volume 15076, pages 222–241, 2024a.

- Omer Belhasin, Yaniv Romano, Daniel Freedman, Ehud Rivlin, and Michael Elad. Principal uncertainty quantification with spatial correlation for image restoration problems. *IEEE Transactions on Pattern Analysis and Machine Intelligence*, 46(5):3321–3333, 2024.
- Zongsheng Yue and Chen Change Loy. Difface: Blind face restoration with diffused error contraction. *IEEE Transactions on Pattern Analysis and Machine Intelligence*, 46(12):9991–10004, 2024.
- Miaoyu Li, Ying Fu, Tao Zhang, Ji Liu, Dejing Dou, Chenggang Yan, and Yulun Zhang. Latent diffusion enhanced rectangle transformer for hyperspectral image restoration. *IEEE Transactions on Pattern Analysis and Machine Intelligence*, 47(1):549–564, 2025.
- Zongsheng Yue, Jianyi Wang, and Chen Change Loy. Efficient diffusion model for image restoration by residual shifting. *IEEE Transactions on Pattern Analysis and Machine Intelligence*, 47(1):116–130, 2025.
- Boyun Li, Xiao Liu, Peng Hu, Zhongqin Wu, Jiancheng Lv, and Xi Peng. All-in-one image restoration for unknown corruption. In *Proceedings of the IEEE/CVF conference on computer vision and pattern recognition (CVPR)*, pages 17431–17441, 2022.
- Vaishnav Potlapalli, Syed Waqas Zamir, Salman H. Khan, and Fahad Shahbaz Khan. Promptir: Prompting for all-in-one image restoration. In *Advances in neural information processing systems (NeurIPS)*, 2023.
- Yuning Cui, Syed Waqas Zamir, Salman H. Khan, Alois Knoll, Mubarak Shah, and Fahad Shahbaz Khan. Adair: Adaptive all-in-one image restoration via frequency mining and modulation. In *International conference on learning representations (ICLR)*, 2025.
- Jinghao Zhang, Jie Huang, Mingde Yao, Zizheng Yang, Hu Yu, Man Zhou, and Feng Zhao. Ingredient-oriented multi-degradation learning for image restoration. In *IEEE/CVF Conference on Computer Vision and Pattern Recognition (CVPR)*, pages 5825–5835, 2023.
- Ziwei Luo, Fredrik K. Gustafsson, Zheng Zhao, Jens Sjölund, and Thomas B. Schön. Controlling vision-language models for multi-task image restoration. In *International conference on learning representations (ICLR)*, 2024.
- Jingbo Lin, Zhilu Zhang, Yuxiang Wei, Dongwei Ren, Dongsheng Jiang, Qi Tian, and Wangmeng Zuo. Improving image restoration through removing degradations in textual representations. In *IEEE/CVF Conference on Computer Vision and Pattern Recognition (CVPR)*, pages 2866–2878, 2024.
- Gang Wu, Junjun Jiang, Yijun Wang, Kui Jiang, and Xianming Liu. Debiased all-in-one image restoration with task uncertainty regularization. In *Proceedings of the AAAI Conference on Artificial Intelligence*, 2025.
- Chu-Jie Qin, Ruiqi Wu, Zikun Liu, Xin Lin, Chun-Le Guo, Hyun Hee Park, and Chongyi Li. Restore anything with masks: Leveraging mask image modeling for blind all-in-one image restoration. In *Proceedings of the european conference on computer vision (ECCV)*, volume 15103, pages 364–380, 2024.
- Syed Waqas Zamir, Aditya Arora, Salman H. Khan, Munawar Hayat, Fahad Shahbaz Khan, Ming-Hsuan Yang, and Ling Shao. Multi-stage progressive image restoration. In *Proceedings of the IEEE/CVF Conference on Computer Vision and Pattern Recognition (CVPR)*, pages 14821–14831, 2021.
- Yuning Cui, Yi Tao, Zhenshan Bing, Wenqi Ren, Xinwei Gao, Xiaochun Cao, Kai Huang, and Alois Knoll. Selective frequency network for image restoration. In *International conference on learning representations (ICLR)*, 2022.
- Xiang Chen, Hao Li, Mingqiang Li, and Jinshan Pan. Learning A sparse transformer network for effective image deraining. In *Proceedings of the IEEE/CVF Conference on Computer Vision and Pattern Recognition (CVPR)*, pages 5896–5905, 2023.

- Qingnan Fan, Dongdong Chen, Lu Yuan, Gang Hua, Nenghai Yu, and Baoquan Chen. A general decoupled learning framework for parameterized image operators. *IEEE Transactions on Pattern Analysis and Machine Intelligence*, 2019.
- Mingde Yao, Ruikang Xu, Yuanshen Guan, Jie Huang, and Zhiwei Xiong. Neural degradation representation learning for all-in-one image restoration. *IEEE Trans. Image Process.*, 33:5408–5423, 2024.
- Marcos V Conde, Gregor Geigle, and Radu Timofte. High-quality image restoration following human instructions. In *European Conference on Computer Vision (ECCV)*, pages 1–12, 2024.
- Pablo Arbeláez, Michael Maire, Charless Fowlkes, and Jitendra Malik. Contour detection and hierarchical image segmentation. *IEEE Trans. Pattern Anal. Mach. Intell.*, 33(5):898–916, 2011.
- Kede Ma, Zhengfang Duanmu, Qingbo Wu, Zhou Wang, Hongwei Yong, Hongliang Li, and Lei Zhang. Waterloo Exploration Database: New challenges for image quality assessment models. *IEEE Trans. Image Process.*, 26(2):1004–1016, Feb. 2017.
- Wenhan Yang, Robby T. Tan, Jiashi Feng, Jiaying Liu, Zongming Guo, and Shuicheng Yan. Deep joint rain detection and removal from a single image. In *Proceedings of the IEEE Conference on Computer Vision and Pattern Recognition (CVPR)*, pages 1685–1694, 2017.
- Boyi Li, Wenqi Ren, Dengpan Fu, Dacheng Tao, Dan Feng, Wenjun Zeng, and Zhangyang Wang. Benchmarking single-image dehazing and beyond. *IEEE Trans. Image Process.*, 28(1):492–505, 2019a.
- Seungjun Nah, Tae Hyun Kim, and Kyoung Mu Lee. Deep multi-scale convolutional neural network for dynamic scene deblurring. In *Proceedings of the IEEE Conference on Computer Vision and Pattern Recognition (CVPR)*, pages 257–265, July 2017.
- Chen Wei, Wenjing Wang, Wenhan Yang, and Jiaying Liu. Deep retinex decomposition for low-light enhancement. In *Proceedings of the british machine vision conference (BMVC)*, page 155, 2018.
- Jeya Maria Jose Valanarasu, Rajeev Yasarla, and Vishal M. Patel. TransWeather: Transformer-based restoration of images degraded by adverse weather conditions. In *Proceedings of the IEEE conference on computer vision and pattern recognition (CVPR)*, pages 2343–2353, 2022.
- Rui Qian, Robby T. Tan, Wenhan Yang, Jiajun Su, and Jiaying Liu. Attentive generative adversarial network for raindrop removal from a single image. In *Proceedings of the IEEE Conference on Computer Vision and Pattern Recognition (CVPR)*, pages 2482–2491, 2018.
- Ruoteng Li, Loong-Fah Cheong, and Robby T. Tan. Heavy rain image restoration: Integrating physics model and conditional adversarial learning. In *Proceedings of the IEEE Conference on Computer Vision and Pattern Recognition (CVPR)*, pages 1633–1642, 2019b.
- Yun-Fu Liu, Da-Wei Jaw, Shih-Chia Huang, and Jenq-Neng Hwang. Desnownet: Context-aware deep network for snow removal. *IEEE Trans. Image Process.*, 27(6):3064–3073, 2018.
- Yu Guo, Yuan Gao, Yuxu Lu, Ryan Wen Liu, and Shengfeng He. Onerestore: A universal restoration framework for composite degradation. In *Proceedings of the european conference on computer vision (ECCV)*, pages 255–272, 2024b.
- He Zhang and Vishal M. Patel. Density-aware single image de-raining using a multi-stream dense network. In *Proceedings of the IEEE Conference on Computer Vision and Pattern Recognition (CVPR)*, pages 695–704, 2018.
- Jingyun Liang, Jiezhong Cao, Guolei Sun, Kai Zhang, Luc Van Gool, and Radu Timofte. SwinIR: Image restoration using swin transformer. In *ICCVW*, pages 1833–1844, 2021.
- Yuning Cui, Wenqi Ren, Xiaochun Cao, and Alois Knoll. Image restoration via frequency selection. *IEEE Trans. Pattern Anal. Mach. Intell.*, 46(2):1093–1108, 2024.
- Lin Liu, Lingxi Xie, Xiaopeng Zhang, Shanxin Yuan, Xiangyu Chen, Wengang Zhou, Houqiang Li, and Qi Tian. TAPE: task-agnostic prior embedding for image restoration. In *Proceedings of the european conference on computer vision (ECCV)*, volume 13678, pages 447–464, 2022.

- Ruoteng Li, Robby T Tan, and Loong-Fah Cheong. All in one bad weather removal using architectural search. In *IEEE/CVF Conference on Computer Vision and Pattern Recognition (CVPR)*, pages 3175–3185, 2020.
- Yurui Zhu, Tianyu Wang, Xueyang Fu, Xuanyu Yang, Xin Guo, Jifeng Dai, Yu Qiao, and Xiaowei Hu. Learning weather-general and weather-specific features for image restoration under multiple adverse weather conditions. In *Proceedings of the IEEE/CVF Conference on Computer Vision and Pattern Recognition (CVPR)*, pages 21747–21758, 2023.
- Ozan Özdenizci and Robert Legenstein. Restoring vision in adverse weather conditions with patch-based denoising diffusion models. *IEEE Trans. Pattern Anal. Mach. Intell.*, 45(8):10346–10357, 2023.
- Tian Ye, Sixiang Chen, Jinbin Bai, Jun Shi, Chenghao Xue, Jingxia Jiang, Junjie Yin, Erkang Chen, and Yun Liu. Adverse weather removal with codebook priors. In *IEEE/CVF International Conference on Computer Vision (ICCV)*, pages 12619–12630, 2023.
- Yuang Ai, Huaibo Huang, Xiaoqiang Zhou, Jiexiang Wang, and Ran He. Multimodal prompt perceiver: Empower adaptiveness, generalizability and fidelity for all-in-one image restoration. In *IEEE/CVF Conference on Computer Vision and Pattern Recognition (CVPR)*, pages 25432–25444, 2024.
- Tian Ye, Sixiang Chen, Wenhao Chai, Zhaohu Xing, Jing Qin, Ge Lin, and Lei Zhu. Learning diffusion texture priors for image restoration. In *IEEE/CVF Conference on Computer Vision and Pattern Recognition (CVPR)*, pages 2524–2534, 2024.
- Shangquan Sun, Wenqi Ren, Xinwei Gao, Rui Wang, and Xiaochun Cao. Restoring images in adverse weather conditions via histogram transformer. In *European Conference on Computer Vision (ECCV)*, volume 15080, pages 111–129, 2024.
- Jia-Bin Huang, Abhishek Singh, and Narendra Ahuja. Single image super-resolution from transformed self-exemplars. In *CVPR*, 2015.
- Rich Franzen. Kodak lossless true color image suite. <http://r0k.us/graphics/kodak/>, 1999. Online accessed 24 Oct 2021.
- David Martin, Charless Fowlkes, Doron Tal, and Jitendra Malik. A database of human segmented natural images and its application to evaluating segmentation algorithms and measuring ecological statistics. In *ICCV*, 2001.

A Additional Experimental Results and Analyses

This section presents supplementary experimental results, including single-task performance benchmarks, out-of-distribution (OOD) generalization analyses, computational complexity comparisons, further iterative inference studies, and additional qualitative results.

A.1 Single-Task Performance Evaluation

To further assess the efficacy of SIPL, we evaluated its performance on individual restoration tasks, aligning our experimental setup with that of PromptIR Potlapalli et al. [2023] and AdaIR Cui et al. [2025]. These evaluations test the capability of our all-in-one model, enhanced with SIPL, on specialized degradation scenarios.

Table 5: Deraining results in the single-task setting on the Rain100L dataset. Our SIPL approach obtains a significant performance boost of 1.98 dB PSNR over baseline PromptIR and 0.12 dB over the AdaIR.

| Method | DIDMDN | UMR | SIRR | MSPFN | LPNet | AirNet | Restormer | PromptIR | AdaIR | PromptIR + SIPL (Ours) |
|--------|--------|-------|-------|-------|-------|--------|-----------|----------|-------|-------------------------------|
| PSNR | 23.79 | 32.39 | 32.37 | 33.50 | 33.61 | 34.90 | 36.74 | 37.04 | 38.90 | 39.02 |
| SSIM | 0.773 | 0.921 | 0.926 | 0.948 | 0.958 | 0.977 | 0.978 | 0.979 | 0.985 | 0.986 |

Deraining on Rain100L: The Rain100L dataset Yang et al. [2017] serves as a standard benchmark for single-image deraining. As presented in Table 5, PromptIR augmented with our SIPL framework achieves state-of-the-art performance. Specifically, it obtains a PSNR of **39.02 dB** and an SSIM of **0.986**. This represents a substantial improvement of **1.98 dB** in PSNR over the original PromptIR baseline and also surpasses the strong AdaIR model by **0.12 dB**, demonstrating the significant benefits of SIPL in effectively removing rain streaks while preserving image fidelity.

Dehazing on SOTS Outdoor: For evaluating dehazing performance, we utilize the outdoor test set from SOTS, part of the RESIDE dataset Li et al. [2019a]. The results in Table 6 indicate that SIPL notably enhances PromptIR’s dehazing capabilities. Our approach (PromptIR + SIPL) achieves a PSNR of **31.82 dB** and an SSIM of **0.982**. This is a gain of **0.51 dB** in PSNR compared to the PromptIR baseline. Furthermore, our method slightly outperforms AdaIR (31.80 dB PSNR / 0.981 SSIM), underscoring SIPL’s efficacy in restoring clarity and detail in hazy conditions.

Denoising using Five-Task Pre-trained Model: To assess robustness and generalization for denoising, we employed the all-in-one model pre-trained on five distinct degradation tasks (including denoising) and evaluated it directly on three commonly used denoising benchmark datasets: Urban100 Huang et al. [2015], Kodak24 Franzen [1999], and BSD68 Martin et al. [2001]. This setup tests the model’s ability to denoise effectively without task-specific fine-tuning. As detailed in Table 7, PromptIR + SIPL demonstrates superior performance, achieving an average PSNR of **31.98 dB** across all datasets and noise levels ($\sigma \in \{15, 25, 50\}$). This is a notable improvement over AdaIR (31.55 dB average PSNR). Particularly on the Urban100 dataset, which often contains complex structures, our method shows significant gains (e.g., **+1.29 dB** for $\sigma = 15$, **+1.06 dB** for $\sigma = 25$). Consistent, positive improvements are also observed across the Kodak24 and BSD68 datasets for all noise levels. These results, especially on datasets potentially unseen during the denoising phase of the five-task training, highlight the advanced robustness and generalization capabilities endowed by the SIPL framework.

Summary of Single-Task Evaluations: The collective results from these single-task evaluations on deraining, dehazing, and denoising consistently underscore the advantages of integrating SIPL with a strong baseline like PromptIR. Across all three distinct restoration tasks, our approach not only yields substantial improvements over the original backbone but also demonstrates competitive or superior performance against recent state-of-the-art methods such as AdaIR. The denoising experiments, in particular, where a versatile five-task model was directly applied to specialized denoising benchmarks, strongly emphasize the generalization power of SIPL. By enabling more effective utilization of learned priors and facilitating self-improvement, SIPL significantly enhances the model’s robustness and its capability to handle diverse image degradations effectively, even when tested in focused, single-task scenarios.

Table 6: Quantitative comparison for single-task dehazing. Our SIPL achieves significant improvement over baseline PromptIR with 0.51 dB PSNR.

| Method | DehazeNet | MSCNN | AODNet | EPDN | FDGAN | AirNet | Restormer | PromptIR | AdaIR | PromptIR + SIPL |
|--------|-----------|-------|--------|-------|-------|--------|-----------|----------|-------|------------------------|
| PSNR | 22.46 | 22.06 | 20.29 | 22.57 | 23.15 | 23.18 | 30.87 | 31.31 | 31.80 | 31.82 |
| SSIM | 0.851 | 0.908 | 0.877 | 0.863 | 0.921 | 0.900 | 0.969 | 0.973 | 0.981 | 0.982 |

Table 7: Image denoising results of directly applying the pre-trained model under the five-degradation setting to the Urban100 Huang et al. [2015], Kodak24 Franzen [1999] and BSD68 Martin et al. [2001] datasets. The results are PSNR scores. Our SIPL achieves significant improvement across all test datasets compared to previous SOTA method AdaIRCui et al. [2025].

| Method | Urban100 | | | Kodak24 | | | BSD68 | | | Average |
|---------------------------------------|---------------|---------------|---------------|---------------|---------------|---------------|---------------|---------------|---------------|--------------|
| | $\sigma = 15$ | $\sigma = 25$ | $\sigma = 50$ | $\sigma = 15$ | $\sigma = 25$ | $\sigma = 50$ | $\sigma = 15$ | $\sigma = 25$ | $\sigma = 50$ | |
| DL Fan et al. [2019] | 21.10 | 21.28 | 20.42 | 22.63 | 22.66 | 21.95 | 23.16 | 23.09 | 22.09 | 22.04 |
| Transweather Valanarasu et al. [2022] | 29.64 | 27.97 | 26.08 | 31.67 | 29.64 | 26.74 | 31.16 | 29.00 | 26.08 | 28.66 |
| TAPE Liu et al. [2022] | 32.19 | 29.65 | 25.87 | 33.24 | 30.70 | 27.19 | 32.86 | 30.18 | 26.63 | 29.83 |
| AirNet Li et al. [2022] | 33.16 | 30.83 | 27.45 | 34.14 | 31.74 | 28.59 | 33.49 | 30.91 | 27.66 | 30.89 |
| IDR Zhang et al. [2023] | 33.82 | 31.29 | 28.07 | 34.78 | 32.42 | 29.13 | 34.11 | 31.60 | 28.14 | 31.48 |
| AdaIR | 34.10 | 31.68 | 28.29 | 34.89 | 32.38 | 29.21 | 34.01 | 31.35 | 28.06 | 31.55 |
| PromptIR + SIPL | 35.39 | 32.74 | 29.17 | 34.98 | 32.50 | 29.36 | 34.08 | 31.45 | 28.16 | 31.98 |

A.2 Out-of-Distribution (OOD) Generalization Analysis

A critical attribute of advanced image restoration models is their capacity to generalize effectively to previously unseen degradation types. This section investigates the OOD generalization capabilities of our SIPL-enhanced framework, drawing comparisons with established methods like PromptIR and AdaIR. Our analysis specifically focuses on performance when encountering complex, composite degradations not present during the training phase.

Performance on Unseen Composite Degradation (Rain100L + Noise): We evaluate models originally trained on three distinct restoration tasks (deraining, dehazing, denoising individually) on a challenging synthetic dataset: Rain100L combined with varying levels of Gaussian noise ($\sigma \in \{15, 25, 50\}$). This composite degradation scenario was deliberately excluded from the training set to rigorously test OOD performance.

The quantitative results are presented in Table 8. Baseline models, PromptIR and AdaIR, achieve average PSNR scores of 24.40 dB and 24.39 dB, respectively, on this unfamiliar task. Our PromptIR + SIPL model, in its initial single-pass inference (“PromptIR + SIPL (initial)”), yields a comparable average PSNR of 24.46 dB. However, the transformative advantage of SIPL becomes strikingly evident through its iterative self-improvement mechanism. With just one iteration (“+Iter 1”), the average PSNR significantly jumps to 25.48 dB. A second iteration (“+Iter 2”) further elevates the performance dramatically to an average PSNR of **29.23 dB**. This represents a remarkable **+4.77 dB** improvement over its initial state and far surpasses the static performance of the baseline models. This progressive and substantial enhancement underscores the robust OOD generalization conferred by SIPL, particularly its ability to iteratively refine results when faced with novel degradations.

The qualitative improvements are visualized in Figure 8 using an example from the Rain100L + Noise ($\sigma = 50$) set. While the input image exhibits significant degradation, and baseline methods like PromptIR and AdaIR offer limited restoration, our SIPL demonstrates clear visual enhancements. The initial output (“SIPL-Init”) shows some improvement, but subsequent iterations (“SIPL-Iter1”, “SIPL-Iter2”) progressively recover finer details, enhance sharpness, and reduce artifacts more effectively, approaching the ground truth quality. This visual evidence corroborates the quantitative gains and highlights the practical efficacy of iterative refinement in complex OOD scenarios.

Efficacy of Self-Improvement in OOD Contexts: The marked success of PromptIR + SIPL in handling these unseen composite degradations, especially through iteration, is attributable to its core design featuring the Privileged Dictionary (PD) and the self-improvement learning strategy. Unlike baseline models such as PromptIR and AdaIR, which are not inherently designed to leverage their own outputs for iterative refinement on OOD tasks without a guiding mechanism, SIPL excels in this regard. Standard architectures, if naively iterated on OOD inputs, might see performance stagnate

Table 8: OOD performance on Rain100L with Gaussian noise ($\sigma = 15, 25$, and 50). Models were trained on three distinct tasks and test on this unseen dataset directly. Iter-N denotes N iterative refinement steps. Best results are underlined, our method is highlighted.

| Method | Rain100L + Gaussian Noise | | | Average |
|-----------------------------------|---------------------------|---------------|---------------|--------------|
| | $\sigma = 15$ | $\sigma = 25$ | $\sigma = 50$ | |
| PromptIR Potlapalli et al. [2023] | 24.92 | 24.50 | 23.79 | 24.40 |
| AdaIR Cui et al. [2025] | 24.91 | 24.50 | 23.77 | 24.39 |
| PromptIR + SIPL (initial) | 24.95 | 24.59 | 23.86 | 24.46 |
| + Iter-1 | 26.90 | 25.59 | 23.96 | 25.48 |
| + Iter-2 | 31.74 | 29.53 | 26.41 | 29.23 |



Figure 8: Visual illustration of OOD performance on a challenging Rain100L + Gaussian Noise ($\sigma = 50$) example. From left to right: Degraded Input, PromptIR, AdaIR, SIPL (Initial), SIPL (Iter 1), SIPL (Iter 2), and Ground Truth (GT). The iterative application of SIPL progressively enhances image clarity, restores fine details, and reduces artifacts, significantly outperforming baseline methods and demonstrating effective generalization to unseen composite degradations.

or even degrade due to the accumulation of errors or model biases when processing unfamiliar data distributions.

In stark contrast, SIPL’s PD, trained to distill essential characteristics of high-quality images, provides robust guidance even when the pseudo-privileged information is derived from an imperfectly restored OOD image. The iterative process allows the model to progressively correct errors and enhance image quality by repeatedly consulting these learned priors. This capacity for effective self-correction and refinement in the face of novel, complex degradations is a key differentiator of our approach.

This OOD analysis strongly suggests that our self-improved iteration paradigm offers a novel and potent pathway for advancing all-in-one image restoration. Beyond striving for optimal performance in a single forward pass, SIPL demonstrates the significant potential of empowering models to adapt and improve their outputs dynamically at test time. This is particularly crucial for real-world scenarios where diverse and unforeseen degradations are common, showcasing a promising direction for developing more versatile and robust restoration solutions.

Table 9: Comparison of model parameters and computational complexity.

| Method | Parameters | FLOPs | Avg. (dB) |
|-----------------------------------------------|------------|-------------|--------------|
| AirNet Li et al. [2022] | 9M | 301G | 25.44 |
| Transweather Valanarasu et al. [2022] | 21.5 | 115.2 | 25.22 |
| PromptIR Potlapalli et al. [2023] | 36M | 173G | 29.15 |
| AdaIR Cui et al. [2025] | 29M | 162G | 30.20 |
| PromptIR + PL | 36M | 173G | 30.05 |
| PromptIR + SIPL (Iter-0 / Single Pass) | 39M | 193G | 30.17 |
| PromptIR + SIPL (Iter-1 / Ours) | 39M | 434G | 30.53 |

A.3 Efficiency Evaluation

We evaluate the parameter count and computational complexity (FLOPs, calculated for a 256×256 input) of our proposed methods against several baselines, alongside their average PSNR performance (dB) on the five-task benchmark. The results are summarized in Table 9.

Our investigation begins with the integration of Privilege Learning (PL) into PromptIR (denoted as “PromptIR + PL”). As a training strategy, PL enhances the model’s learning for multi-degradation

scenarios. Notably, this approach achieves an average PSNR of 30.05 dB. Comparing to the baseline PromptIR (29.15 dB), this represents an improvement of 0.9 dB. Critically, this performance boost is achieved while maintaining the original model’s parameter count (36M) and FLOPs (173G) during inference, as PL primarily modifies the training process. This underscores PL’s efficacy as a zero-cost inference enhancement for all-in-one image restoration.

Building upon this, our Self-Improved Privilege Learning (SIPL) framework, even in a single pass (“PromptIR + SIPL (Iter-0)”), yields further performance gains, reaching 30.17 dB. This increment validates the effectiveness of our proposed Privileged Dictionary (PD) within the Proxy Fusion module. The PD successfully captures essential structural information during training and, crucially, retains this privileged knowledge for inference, thereby extending the conventional PL paradigm. The introduction of the Proxy Fusion module and the privileged feature handling results in a marginal increase of 3M parameters and 20G FLOPs over the “PromptIR + PL” model. This is because the acquisition of privileged features for Proxy Fusion is efficient, primarily leveraging encoder-level features rather than requiring full model duplication for the privileged path.

The true potential of SIPL is unlocked through iterative inference (“PromptIR + SIPL (Iter-1)”), which achieves a higher PSNR of 30.53 dB, demonstrating self-driven performance enhancement. We acknowledge that this iterative process leads to a considerable increase in computational load (434G FLOPs) compared to single-pass models. However, this increased cost is often justified by the substantial and consistent performance improvements observed across diverse restoration tasks and, significantly, in challenging Out-of-Distribution (OOD) scenarios as detailed in Section A.2. The self-improved iteration capability provides a powerful form of test-time adaptation, offering a highly effective solution for handling unknown or complex composite degradations in the all-in-one image restoration landscape.

Looking ahead, while the current iterative framework demonstrates compelling results, future research will focus on optimizing its efficiency. We plan to explore avenues such as simplifying the overall design, potentially by identifying and leveraging key model weights more selectively. Further investigation into using the Privileged Dictionary more sparsely within specific feature spaces could also reduce the computational demands of the privileged feature fusion process, aiming to strike an even better balance between performance and efficiency.